

## Large Electric Field Effect in Electrolyte-Gated Manganites

Anoop Singh Dhoot,<sup>1</sup> Casey Israel,<sup>2</sup> Xavier Moya,<sup>2</sup> Neil D. Mathur,<sup>2</sup> and Richard Henry Friend<sup>1</sup>

<sup>1</sup>*Cavendish Laboratory, JJ Thomson Avenue, Cambridge CB3 0HE, United Kingdom*

<sup>2</sup>*Department of Materials Science and Metallurgy, University of Cambridge, Pembroke Street, Cambridge CB2 3QZ, United Kingdom*

(Received 19 December 2008; published 30 March 2009)

We have studied electrostatic field-induced doping in  $\text{La}_{0.8}\text{Ca}_{0.2}\text{MnO}_3$  transistors using electrolyte as a gate dielectric. For positive gate bias, electron doping drives a transition from a ferromagnetic metal to an insulating ground state. The thickness of the electrostatically doped layer depends on bias voltage but can extend to 5 nm requiring a field doping of  $2 \times 10^{15}$  charges per  $\text{cm}^2$  equivalent to 2.5 electrons per unit cell area. In contrast, negative gate voltages enhance the metallic conductivity by 30%.

DOI: 10.1103/PhysRevLett.102.136402

PACS numbers: 71.30.+h, 73.61.-r, 75.47.Lx

Brattain and fellow inventors of the bipolar transistor were the first to use electrolyte gate dielectrics to realize very high field-induced carrier densities in the conducting channel of a field-effect transistor (FET) [1]. Since switching the state of the transistor requires ionic motion, such devices would inevitably be slow and therefore unattractive for practical applications. There has, however, been recent interest in the use of electrolytes to gate field-effect structures made with molecular semiconductors [2], with clear evidence for very high increases in conductivity introduced into otherwise semiconducting materials [3]. There is some debate as to whether this change in conductivity is due to a “pure” field effect or whether there is some movement of ions into the bulk of the semiconductor (electrochemical doping—a well-established process for these materials). There has been very little effort to extend this approach to inorganic materials [4], and we present here studies of such structures built with the colossal magnetoresistive manganites.

Since the discovery of colossal magnetoresistance in the manganites [5], there has been interest in using FETs to induce sufficiently high field-induced carrier density in the conducting channel to control the metal to insulator transition [6,7]. Nominally large changes in the Curie temperature  $T_C$  of up to 34 K have been reported for manganite transistors made using ferroelectric gate dielectrics, which can support high carrier densities ( $\sim 10^{14} \text{ cm}^{-2}$ ) in the transistor channel [8]. More recently,  $T_C$  modulation of 43 K has been shown in devices made using  $\text{SrTiO}_3$  as the gate dielectric [9]. However, use of the field effect in all-oxide devices is limited by the capacitance and electric field breakdown strength of the gate dielectric and is generally restricted to systems with limited lattice mismatch that generate limited strain.

We use here the ionic liquid 1-ethyl-3-methylimidazolium bis(trifluoromethylsulfonyl)imide (EMIM:TFSI) and poly(ethylene oxide)/lithium perchlorate (PEO/ $\text{LiClO}_4$ ) polymer electrolyte [10] as the gate dielectric. Figure 1(a) shows the device structure used including the electrolyte gate dielectric. Epitaxial thin films of the manganite  $\text{La}_{0.8}\text{Ca}_{0.2}\text{MnO}_3$  (LCMO) were used here because

they show good stability in air at room temperature and have a magnetic phase transition at a temperature below that at which the ions in the electrolyte are immobile [11]. We note that Itoh *et al.* have shown evidence for room temperature electrochemical reduction of manganite samples in contact with propylene carbonate electrolyte, with consequent modification of  $T_C$  [12]. Changes in the stoichiometry of the samples caused by chemical or electrochemical reactions are undesirable, and careful consideration of capacitive and doping effects must be made to determine the extent to which this occurs.

We find a voltage-induced metal to insulator phase transition in electrolyte-gated manganite films. For a film thickness of 5 nm and positive gate voltage, there is complete electrostatic doping of the whole thickness from ferromagnetic metal to insulator, not reported before for manganites. Analysis of the data reveals that the film conductance is well described by a simple linear sum of the conductances of fully field-doped insulating and underlying metallic layers.

The electrolyte function is shown in Fig. 1(a): For positive gate voltage  $+V_g$ , electrons are induced in the conducting channel of the device by cations ( $\text{EMIM}^+$  or

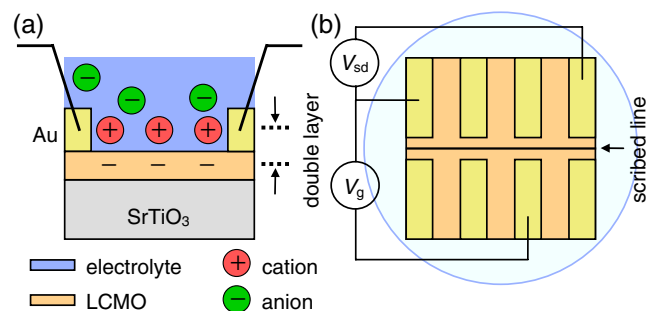


FIG. 1 (color online). Schematic drawing of the field-effect device showing a possible arrangement of the ionic double layer (a) for positive applied  $V_g$ , and top view (b) of the diamond scribed thin film covered in electrolyte. The gate voltage was applied to the electrolyte using a probe placed on the other half of the inorganic film.

$\text{Li}^+$ ) absorbed directly onto the manganite surface; similarly, carriers of opposite sign (holes) are induced in the channel for negative gate voltage  $-V_g$ . To maintain double layer formation in our experiments,  $V_g$  was applied to the electrolyte and held constant while cooling the sample to a temperature low enough to prevent further ionic motion. This temperature was typically below 250 K for our electrolytes.

The LCMO films were grown by pulsed laser deposition ( $\lambda = 248$  nm, 1 Hz, 2.0 J per  $\text{cm}^2$ , 850 °C, 15 Pa of flowing  $\text{O}_2$ , target substrate = 8 cm) from a stoichiometric target (Praxair) on a polished  $\text{SrTiO}_3$  (001) substrate and annealed *in situ* ( $\sim 50$  kPa  $\text{O}_2$ , 750 °C, 0.5 h) before cooling (10 °C per min) to room temperature. Thickness was determined from film fringes in an  $\omega$ - $2\theta$  x-ray scan about  $\text{SrTiO}_3$  (002) taken with a Philips X'Pert diffractometer ( $\lambda = 1.54$  Å). Devices were metallized by thermal evaporation of  $\approx 75$  nm Au and a 5 nm thick Cr adhesion layer. The channel length was 2.5 mm, and the channel width was  $\approx 2$  mm. We use a standard four-probe configuration to avoid contact resistance by placing two long parallel electrodes, each 0.5 mm wide and the same apart, between the source and drain electrodes. The manganite layer was scribed using a diamond tip into two roughly equal but separate areas, and  $V_g$  was applied between an additional fifth electrode and one of the outer electrodes [Fig. 1(b)]. Ionic liquid or polymer electrolyte [3] was deposited directly onto the manganite layer covering both sides of the scribed line. Devices were measured using Keithley 2612 and 2400 source-measure units. Temperature was varied from 298 to 4.2 K by lowering the device into liquid helium and raising back up again. The magnitude of the maximum current flowing through the conducting channel was  $\sim 10$   $\mu\text{A}$ .

Figure 2(a) shows the temperature dependence of the resistance for an ionic liquid gated manganite device with film thickness of 5 nm for two different  $V_g$  (+1 V and -1 V [13]) with each polarization voltage being first applied to the electrolyte at room temperature. The gate electrode was disconnected below 250 K (below the melting point of EMIM:TFSI, 258 K). For all applied  $V_g$ , we find  $dR/dT < 0$ , at high  $T$ , followed by a change in slope and metallic transport  $dR/dT > 0$ , at low  $T$ , consistent with a transition from the insulating (paramagnetic) to metallic (ferromagnetic) ground state. The fractional change in conductance relative to  $V_g = 0$  V,  $[G_s(V_g) - G_s(0 \text{ V})]/G_s(0 \text{ V})$ , gives a maximum absolute value of  $\Delta G_s/G_s = 74\%$  (30%) for  $V_g = +1$  V (-1 V). For  $T \approx T_C$  and higher, the channel conductance clearly increases (decreases) for negative (positive)  $V_g$ , similar in all practical respects to the operation of a *p*-type transistor.

Although, strictly,  $T_C$  is obtained from the magnetic transition, carrier transport closely follows the magnetic property, typically to within a few degrees Kelvin [11], so that at  $V_g = 0$  V,  $T_C$  is close to the resistance maximum at

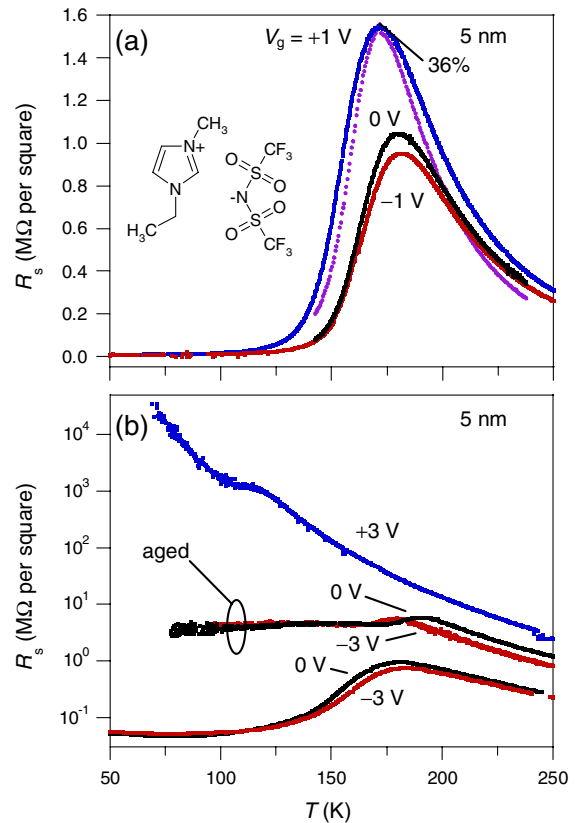


FIG. 2 (color online). Sheet resistance versus temperature for a device with a 5 nm thick LCMO layer gated with the ionic liquid EMIM:TFSI (a) at  $V_g = 0$  (black line),  $-1$  (red line), and  $+1$  V (blue line), with  $V_{sd} = -0.1$  V. The data at  $V_g = +1$  V are fit to a parallel circuit model (purple line). The calculated field-induced insulating fraction of the film resistance (at the resistance maximum) is indicated. The inset shows the molecular structure of the ionic liquid. Resistance data for another 5 nm thick film device (b) at  $V_g = 0$  (black line),  $-3$  (red line), and  $+3$  V (blue line). Data for the aged device for  $V_g = 0$  V and  $V_g = -3$  V recorded immediately after the  $V_g = +3$  V run are also shown. For (b)  $V_{sd} = -0.1$  V, except for  $V_g = +3$  V, where  $V_{sd} = -10$  V.

180 K. In contrast, with an applied gate bias, the measured resistivity results from the parallel circuit of manganite layers close to the electrolyte that are “field-doped” and those layers further away that are unaffected. Though there appears to be a continuous shift of the resistance maximum to 181 and 172 K for  $V_g = -1$  and  $+1$  V, respectively, as shown below, this results from a fully doped now insulating layer in parallel with unchanged layers in the bulk.

Figure 2(b) shows resistance data for another device with a 5 nm thick manganite layer (prepared in the same deposition run) gated at larger  $V_g$ . For  $V_g = +3$  V, the data show no clear resistance maximum. Instead, we find a monotonic increase in  $R_s$  for decreasing  $T$ , characteristic of an insulator. The magnitude of the field effect is clearly dependent on the sign of the gate voltage used, with the

change in conductivity for  $+V_g$  orders of magnitude larger than that found in all-oxide transistors. This substantial change in conductivity indicates substantial difference in band filling and hence charge density induced in the thin manganite film.

Figure 3(a) shows the resistance data for a polymer electrolyte-gated device, for  $V_g = +3$  and  $-3$  V. The data show that the resistance maximum is at 190 and 158 K for  $V_g = -3$  and  $+3$  V, respectively. The fractional change in conductance gives a maximum absolute value of  $\Delta G_s/G_s = 100\%$  (23%) for  $V_g = +3$  V ( $-3$  V). This resistivity behavior is similar to that found using the ionic liquid as the gate but with weaker modulation of  $R_s$  for the same applied  $V_g$ .

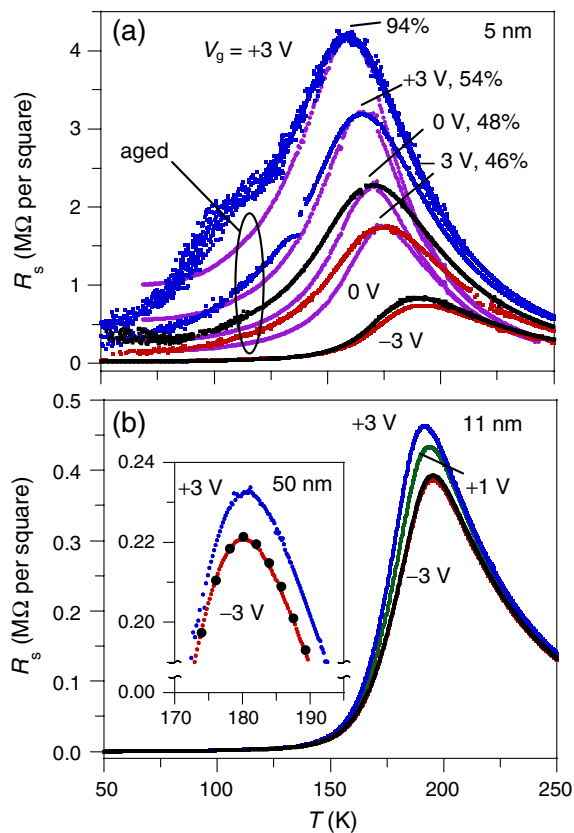


FIG. 3 (color online). Sheet resistance versus temperature for a polymer electrolyte-gated device with LCMO layer thickness of 5 nm (a) at  $V_g = 0$  (black line),  $-3$  (red line), and  $+3$  V (blue line), with  $V_{sd} = -0.1$  V (except for  $V_g = +3$  V, where  $V_{sd} = -0.5$  V). The data for the aged device are also shown ( $V_{sd} = -0.5$  V for  $V_g = 0$  and  $-3$  V, and  $V_{sd} = -10$  V for  $V_g = +3$  V). Data for  $V_g > 0$  V are fitted to the parallel circuit model (purple line). The field-induced insulating fraction is indicated. Device with LCMO thickness of 11 nm (b) at  $V_g = 0$  (black line),  $-3$  (red line),  $+1$  (green line), and  $+3$  V (blue line). The inset shows the data for a device with LCMO layer thickness of 50 nm at  $V_g = 0$  (filled circles),  $-3$ , and  $+3$  V. For (b) and the inset,  $V_{sd} = -0.1$  V.

The monotonic increase in  $R_s$  with  $T$  at  $V_g = +3$  V shown in Fig. 2(b) is similar to that found for the insulating antiferromagnetic end member  $\text{LaMnO}_3$  [14], with a Néel temperature  $T_N \approx 140$  K [11], implying a fully field-doped layer with complete conversion of the film thickness into insulating  $\text{MnO}_3$  sheets. We can reconstruct the resistance curves measured for  $+V_g$  using a simple weighted sum of the conductance measured at  $V_g = +3$  V [Fig. 2(b)] and that measured at  $V_g = 0$  V for the ungated device. We clearly see from Figs. 2 and 3 that the continuous variation in the resistance maximum for varying  $V_g$  is well tracked by such a linear superposition. Similar analysis of all of our devices revealed the same parallel circuit behavior. We calculate the fraction of the resistive layer that is insulating at the resistance maximum to be 36% ( $V_g = +1$  V) and 94% ( $V_g = +3$  V) for the ionic liquid and polymer electrolyte as the gate in Figs. 2(a) and 3(a), respectively.

A basic issue for these structures is the thickness of the field-induced charge layer for which substantial charge density is induced. Our observations provide two experimental clarifications. First, we note that the increase in resistance (between  $V_g = 0$  and  $+3$  V) is as much as a factor of  $10^5$  at 75 K [Fig. 2(b)]. This strongly indicates that the thickness below the electrolyte gate that has been “electrostatically doped” extends through most of the nominal film thickness (5 nm), or else there would be a shunt. Second, we observe that thicker films [as shown in Fig. 3(b)] show an increase of the resistance for positive  $V_g$  near the bulk ferromagnetic transition at  $\approx 195$  and 180 K ( $V_g = 0$  V) for 11 and 50 nm films, respectively. For  $V_g = +3$  V, conductance is decreased by up to 29% in the 11 nm film and by 7.6% for the 50 nm film. If we take the electrostatically doped layer to show the same resistivity behavior as the 5 nm film at  $V_g = +3$  V [Fig. 2(b)], the resistivity of this layer near  $T_C$  is therefore increased significantly with respect to the bulk material. A simple parallel circuit for the bulk and field-doped layers then gives a lower limit to the channel thickness of 3.2 and 3.8 nm for the 11 and 50 nm films, respectively.

These observations indicate that the thickness of the charge-induced layer (for  $+V_g$ ) is substantial, much larger than the very low values that might be expected for Thomas-Fermi screening from a high carrier density metal. However, the particular manganite composition we have used here has a limited charge storage capacity for electrons because the conduction band is split by a large Jahn-Teller energy of 0.5–1.5 eV [11]. We note that, for  $+V_g$ , electrons are injected into the manganite layer, “neutralizing” the effect of the hole doping caused by  $\text{Ca}^{2+}$  substitution of  $\text{La}^{3+}$ . The maximum electron injection is therefore 0.2 electrons per  $\text{MnO}_3$  unit cell (of height  $\approx 0.39$  nm). At this “undoped” limit, we expect an insulator, consistent with the substantial increase in resistance seen in Figs. 2 and 3. This insulating layer is not then able

to provide electrostatic screening, so further manganite layers will be charged in sequence. If all layers in the 5 nm thick film are similarly electrostatically doped to this level, then we require about 2.5 electronic charges per  $\text{MnO}_3$  unit cell—a high but physically reasonable number. We note that, for  $-V_g$ , the maximum level of hole injection is 0.8 holes per unit cell, which corresponds to a thickness for the field-doped layer that is 4 times smaller than that for  $+V_g$ , consistent with the dependence of the field effect on the sign of the gate voltage used.

In our simple parallel circuit model, we have two separate layers: (i) a fully field-doped layer extending from the electrolyte-manganite interface towards the  $\text{SrTiO}_3$  substrate and (ii) the underlying, ungated layer with  $T_C$  of 180–195 K. The thickness and conductance of the gated and ungated layers depend on the applied  $V_g$ . At low temperatures, i.e.,  $T < T_C$ , one can expect the insulating and ferromagnetic layers to give little layer-to-layer coupling, further suppressing the ferromagnetic metallic state (in the unaddressed under layer). For  $T > T_C$ , the gated and ungated layers are in the same paramagnetic (insulating) ground state. We note that the data show a clear change in slope at  $T \approx 105$  K and  $V_g = +3$  V for a manganite layer of thickness 5 nm, which is not present for lower voltages (or thicker films). This may be associated with the structural phase transition in  $\text{SrTiO}_3$  that occurs near this temperature [15], consistent with minimal thickness for any “dead layer” in the device.

Finally, though the field effect is reversible, with time in contact with electrolyte, and with repeated cycling, the change in conductance for  $V_g = +3$  V (and  $V_g = -3$  V) becomes smaller. This is illustrated in Fig. 3(a), where we show data for an aged device (data were recorded after three consecutive cooling and warming cycles of about 3 hours total duration). We calculate that the fraction of the film that is insulating at  $V_g = +3$  V decreases from 94% to 54% upon aging. Similarly, for the device shown in Fig. 2(b), we find only partial recovery of the original  $R_s$  value by repolarization of the electrolyte at  $V_g = 0$  and  $-3$  V. We can speculate that such degradation is caused by the presence of impurities such as water (from the ambient atmosphere) that take part in electrochemical reactions at the metal electrodes, for example. There is also the possibility of electric field-driven movement of dopant atoms in the transistor channel. This could proceed by either electromigration of mobile oxygen ions inside the lattice or insertion of dopant atoms followed by subsequent rearrangement (reordering) of the atomic structure. We rule

out electromigration given the slow ionic diffusion rates typical in manganites at room temperature, particularly in stoichiometric samples containing a relatively small fraction of vacant dopant sites [16]. However, while the interstitial insertion of the larger ions of the ionic liquid into the manganite film is unlikely, insertion of the small  $\text{Li}^+$  cation for  $+V_g$  is difficult to rule out completely.

We have shown voltage-induced modulation of the conductivity in electrolyte-gated colossal magnetoresistive thin films. Very high field-induced carrier densities in the transistor channel drive a metal to insulator phase transition. The electrostatically field-doped layer is shown to extend  $\approx 5$  nm into the film thickness, with a corresponding areal density of  $2 \times 10^{15}$  carriers per  $\text{cm}^2$ . A simple parallel circuit of gated and ungated layers can be used to model the film resistance in devices. An exciting opportunity is created for use of electrolyte as the gate dielectric in a wide variety of inorganic materials to explore formerly inaccessible band-filling regimes without the need for chemical substitution and associated disorder.

A. S. D. thanks The Leverhulme Trust and Isaac Newton Trust for financial support. X. M. acknowledges support from Comissionat per a Universitats i Recerca del Departament d’Innovació, Universitats i Empresa de la Generalitat de Catalunya and EU FP6 STREP CoMePhS.

- 
- [1] W. H. Brattain and C. G. B. Garrett, *Bell Syst. Tech. J.* **34**, 129 (1955).
  - [2] J. H. Cho *et al.*, *Nature Mater.* **7**, 900 (2008).
  - [3] A. S. Dhoot *et al.*, *Proc. Natl. Acad. Sci. U.S.A.* **103**, 11 834 (2006).
  - [4] K. Ueno *et al.*, *Nature Mater.* **7**, 855 (2008).
  - [5] S. Jin *et al.*, *Science* **264**, 413 (1994).
  - [6] S. Mathews *et al.*, *Science* **276**, 238 (1997).
  - [7] T. Wu *et al.*, *Phys. Rev. Lett.* **86**, 5998 (2001).
  - [8] X. Hong *et al.*, *Phys. Rev. B* **68**, 134415 (2003).
  - [9] I. Pallecchi *et al.*, *Phys. Rev. B* **78**, 024411 (2008).
  - [10] P. G. Bruce and C. A. Vincent, *J. Chem. Soc., Faraday Trans.* **89**, 3187 (1993).
  - [11] J. M. D. Coey, M. Viret, and S. V. Molnar, *Adv. Phys.* **48**, 167 (1999).
  - [12] M. Itoh *et al.*, *Solid State Commun.* **97**, 179 (1996).
  - [13] For this (and only this device), Au was deposited on one-half of the LCMO layer and used as the gate electrode.
  - [14] M. Viret, L. Ranno, and J. M. D. Coey, *Phys. Rev. B* **55**, 8067 (1997).
  - [15] M. Egilmez *et al.*, *Phys. Rev. B* **78**, 172405 (2008).
  - [16] L. Malavasi *et al.*, *Solid State Commun.* **123**, 321 (2002).